Video Article

Using Neutron Spin Echo Resolved Grazing Incidence Scattering to Investigate Organic Solar Cell Materials

Andrew J. Parnell[1], Adam Hobson[2], Robert M. Dalgliesh[3], Richard A. L. Jones[1], Alan D. F. Dunbar[2]

[1]Department of Physics and Astronomy, University of Sheffield

[2]Department of Chemical and Biological Engineering, The University of Sheffield

[3]ISIS Pulsed Neutron and Muon Source Science and Technology Facilities Council, Rutherford Appleton Laboratory

Correspondence to: Alan D. F. Dunbar at a.dunbar@sheffield.ac.uk

URL: http://www.jove.com/video/51129
DOI: doi:10.3791/51129

Keywords: Physics, Issue 83, Spin Echo Resolved Grazing Incidence Scattering, Neutron, Crystallite, Organic solar cell, PCBM, P3HT

Date Published: 1/15/2014

Citation: Parnell, A.J., Hobson, A., Dalgliesh, R.M., Jones, R.A.L., Dunbar, A.D.F. Using Neutron Spin Echo Resolved Grazing Incidence Scattering to Investigate Organic Solar Cell Materials. *J. Vis. Exp.* (83), e51129, doi:10.3791/51129 (2014).

Abstract

The spin echo resolved grazing incidence scattering (SERGIS) technique has been used to probe the length-scales associated with irregularly shaped crystallites. Neutrons are passed through two well defined regions of magnetic field; one before and one after the sample. The two magnetic field regions have opposite polarity and are tuned such that neutrons travelling through both regions, without being perturbed, will undergo the same number of precessions in opposing directions. In this case the neutron precession in the second arm is said to "echo" the first, and the original polarization of the beam is preserved. If the neutron interacts with a sample and scatters elastically the path through the second arm is not the same as the first and the original polarization is not recovered. Depolarization of the neutron beam is a highly sensitive probe at very small angles (<50 μrad) but still allows a high intensity, divergent beam to be used. The decrease in polarization of the beam reflected from the sample as compared to that from the reference sample can be directly related to structure within the sample.

In comparison to scattering observed in neutron reflection measurements the SERGIS signals are often weak and are unlikely to be observed if the in-plane structures within the sample under investigation are dilute, disordered, small in size and polydisperse or the neutron scattering contrast is low. Therefore, good results will most likely be obtained using the SERGIS technique if the sample being measured consist of thin films on a flat substrate and contain scattering features that contains a high density of moderately sized features (30 nm to 5 μm) which scatter neutrons strongly or the features are arranged on a lattice. An advantage of the SERGIS technique is that it can probe structures in the plane of the sample.

Video Link

The video component of this article can be found at http://www.jove.com/video/51129/

Introduction

The SERGIS technique aims to be able to yield unique structural information not accessible using other scattering or microscopy techniques from thin film samples. Microscopy techniques are typically surface limited or require significant alteration/sample preparation to view internal structures. Conventional scattering techniques such as reflectivity can provide detailed information about buried sample structures as a function of depth within the thin film but cannot probe structure in the plane of the thin film easily. Ultimately it is hoped that SERGIS will enable this lateral structure to be probed even when buried within the thin film sample. The representative results presented here demonstrate that it is possible to observe a SERGIS signal from irregular sample features and that the measured signal can be correlated with a characteristic length scale associated with the features present in the sample, as confirmed by conventional microscopy techniques.

Inelastic spin echo techniques were developed by Mezei *et al.*[1] in the 1970s. Since then the SERGIS technique (which is an extension of the ideas of Mezei *et al.*) has been successfully demonstrated experimentally using a variety of samples such as highly regular diffraction gratings[2-6] and circular de-wetted polymer droplets[7]. A dynamical theory has been developed by Pynn and coworkers to model the strong scattering from highly regular samples[3-6,8]. This work has highlighted many practical aspects to be considered when performing this type of measurement and has led to a constant dialogue within a small multinational community.

Good results from SERGIS experiments will most likely be obtained if the sample being measured consists of a thin film on a flat substrate and contains scattering features with a high density of moderately sized features (30 nm to 5 μm) that scatter neutrons strongly, as demonstrated by the authors[9]. Unlike other established reflectivity techniques that probe the sample as a function of depth, the SERGIS technique has the advantage that it can probe structures in the plane of the sample surface. Furthermore, the use of spin-echo removes the requirement to tightly collimate the neutron beam in order to obtain either high spatial or energy resolution, consequently significant flux gains can be achieved. This is particularly relevant for grazing incidence geometries that are significantly flux limited because of the need to collimate the beam strongly in

Copyright © 2014 Journal of Visualized Experiments

one direction. Using the OffSpec instrument it should therefore be possible to probe length scales from 30 nm to 5 μm in both bulk and surface structures.

Protocol

1. Sample Preparation

1. Clean the silicon substrates by placing 2 in silicon wafers that are 4 mm thick in oxygen plasma for 10 min.
2. Spincoat the first layer on the substrates
    1. Filter the poly(3,4-ethylenedioxythiophene): poly(styrenesulfonate) (PEDOT:PSS) through a 0.45 μm PTFE filter (PALL).
    2. Use approximately 0.5 ml for each sample to spin coat a PEDOT:PSS thin film onto the two clean substrates at 5,000 rpm spinning for 60 sec.
    3. Dry each substrate for 10 min in an oven at 70 °C.
3. Prepare the blend solution for the second layer
    1. Dissolve some poly(3-hexylthiophene-2,5-diyl) (P3HT) in chlorobenzene at a concentration of 50 mg/ml.
    2. Prepare a solution of PCBM also in chlorobenzene at a concentration of 50 mg/ml.
    3. Mix the two solutions in a proportion of 1:0.7 P3HT:PCBM.
    4. Filter the mixed solution through a 0.45 μm PTFE filter.
4. Spincoat second layer by depositing approximately 100 μl of the P3HT:PCBM solution onto the PEDOT:PSS coated substrates and then spin at 2,000 rpm for 30 sec to form the second layer.
5. Leave one sample as cast and thermally anneal the other for 1 hr at 150 °C in an oven. This results in the growth of the large PCBM crystallites on the thin film surface.

2. Sample Characterization by Microscopy

1. Optical microscopy
    1. Take an optical microscopy image of both samples using a 40X microscope objective on an optical microscope operating in reflection mode, capturing the images using a CCD camera.
    2. Record a calibration image of a sample of known length at the same magnification used for the step 2.1.1
    3. Calculate the pixel size in microns for the images by determining the number of pixels for the sample of known size.
    4. Use this know pixel size to calibrate the images using any readily available microscopy software. An example of a calibrated optical microscopy image is shown in **Figure 1**.
2. Atomic Force Microscopy
    1. Take an atomic force microscope (AFM) image of the two samples.
    2. Analyze the data using any readily available scanning probe software to generate line profile figures like those presented in **Figure 1**.

3. SERGIS Experiment

1. Select a suitable reference sample to provide the reference polarization P_0, which enables the data acquired from the sample of interest data to be normalized.
2. Align the sample and reference sample
    1. Place all three samples on a positioning table; this can be translated across the neutron beam so each sample can be placed in the beam in turn.
    2. Position the P_0 reference sample in the beam by translating the sample table.
    3. Align the P_0 reference sample to an angular accuracy of <0.005° using standard reflection alignment methods.
    4. Place the sample of interest in the neutron beam by translating the sample table.
    5. Align both the sample of interest to an angular accuracy of <0.005° using standard reflection alignment methods.
    6. Repeat this alignment process for all samples of interest to be measured.
3. Tune the SERGIS instrument so it is in echo mode
    1. Set up the dedicated off-specular reflectometer OffSpec at the ISIS Pulsed Neutron and Muon Source (Oxfordshire, UK) to produce wavelengths from 2-14 Å. Further details of the set up used can be found here[10].
    2. Tune the instrument to balance the total number of neutron precessions in each arm of the instrument by scanning the current in part of the guide field arrangement. This is achieved by setting the strength and inclination of the magnetic fields within the encoding arms of the instrument, which are defined by the distance between the RF spin flippers.
4. Set the angle of grazing incidence by tilting the sample table so the neutron beam is incident upon the P_0 sample (for this experiment at an angle of 0.3°).
5. Block the directly transmitted neutron beam from reaching the detector in order to prevent saturation problems.
6. Measure the samples
    1. Move the sample translation stage so the reference sample is once again in the neutron beam and measure the scattered neutron intensity as a function of position on a vertically oriented linear scintillator detector for the reference sample. Measure both spin up and spin down orientations by flipping the spin of the scattered beam immediately before the analyzer. Typically this is done for a period of about 1 hr. This enables the polarization to be determined as well as the scattered intensity for both settings.

2. Translate the sample stage so as to measure the first of the samples of interest, again recording both spin up and spin down orientations as a function of position using a vertically oriented linear scintillator detector for a period of about 1 hr.
3. Repeat steps 3.6.1 and 3.6.2 until sufficiently good counting statistics for this measurement have been obtained. Typically this is about 8 hr/sample in total.
4. Repeat steps 3.6.1-3.6.3 for any further samples that need to be measured.

7. The collected data consists of both spin up and spin down 2D intensity maps for each sample. Calculate the polarization for each pixel in the 2D data sets by using the formula

$$P = \frac{I_{Up} - I_{Down}}{I_{Up} + I_{Down}}$$

where P is the polarization and I_{up} and I_{down} are the measured spin up and spin down intensities respectively.

8. Normalize the data sets acquired for the samples of interest using the P_0 reference sample data collected to produce a normalized polarization intensity map according to the formula

$$P_{Normalised} = \frac{P_{Sample}}{P_0}$$

where $P_{Normalized}$ is the determined polarization calculated and P_{Sample} is the sample polarization value and P_0 is the polarization measured using the P_0 reference sample.

9. Integrate the SERGIS data over a suitable range
   1. Select the area (*i.e.* the pixel range in the normalized polarization plot) for the SERGIS data integration. This area should be selected so as to avoid swamping the desired SERGIS signal by any potential polarization inhomogeneities resulting from imperfections in the field line-integrals. The available Q space that the SERGIS signal may be integrated over is effectively limited to a series of discrete Q values at any given spin-echo length configuration, where Q is the momentum transfer vector *i.e.* the change in momentum of a neutron after interacting with the sample
   2. Reduce the 2D data by integrating the normalized polarization to get the SERGIS correlation function G(y) which has been defined previously[5]. Strictly G(y) should be integrated to infinity over both Q vectors perpendicular to y, however, for experimental reasons the integration area is limited to selected detected intensity above the sample horizon.

10. Compensate for different scattering length densities at different wavelengths by treating the data in a similar manner to spin echo small angle neutron scattering data by plotting the data in the form:

$$\frac{\ln\left(P_{Sample}(\lambda) / P_0(\lambda)\right)}{\lambda^2}$$

where λ is the spin echo length in nm and may be readily calculated using $y = \alpha\lambda^2$, where α is a constant determined using calibrated constants for the given instrument setup[11].

Representative Results

The representative results from samples of [6,6]-phenyl-C61-butyric acid methyl ester (PCBM) and poly(3-hexylthiophene-2,5-diyl) (P3HT) presented here are of significant interest because of their widespread application as bulk hetero-junction materials in organic photovoltaic cells[12,13]. Typically during the fabrication of an organic photovoltaic device, a P3HT:PCBM blend solution is spin-cast from a blend solution to form a thin film on a poly(3,4-ethylenedioxythiophene):poly(styrenesulfonate) (PEDOT:PSS) coated transparent anode (commonly indium tin oxide). The resulting thin film is then coated in a metallic layer which forms the cathode by evaporation. The entire device is then annealed and encapsulated. There is significant interest in understanding how the annealing process affects the phase separation of the P3HT and PCBM and any subsequent PCBM crystallite growth which may occur within the device upon annealing because P3HT:PCBM organic photovoltaic devices are typically thermally annealed to enhance the device efficiency[12,13,14]. Extensive thermal annealing can result in large irregular PCBM crystallites forming on the surface of the blend layer; these could have significant impact upon device performance by denuding PCBM from the blend film and disrupting the metal cathode.

The representative results show that it is possible to use the SERGIS technique to probe the length-scales associated with crystallites of [6,6]-phenyl-C61-butyric acid methyl ester which decorate the surface of a thin film cast from a blend of P3HT:PCBM. The SERGIS signal from an as-cast P3HT:PCBM thin film on a PEDOT:PSS coated silicon substrate and a similar sample which has been extensively annealed. The as-cast sample has a smooth flat surface as shown in **Figure 1(a)** but large crystallites of PCBM develop on the surface upon prolonged thermal annealing as shown in **Figure 1(b)**.

Figure 2 shows the data 2D neutron scattering intensity measured for the annealed P3HT:PCBM sample at one fixed spin echo setting (spin up) using OffSpec in the manner described in this procedure. The off specular scattering of interest to be in analyzed in these experiments is superimposed upon the neutron scattering observed in a conventional specular reflectivity experiment. The intensity of the specular reflectivity will have an intensity value of unity in the total reflection regime but then decays rapidly as a function of Q by six orders of magnitude or more. Other off-specular features are typically 100-1,000 times weaker than the specular signal and are located at well-defined positions in Q space.

Figure 3 shows the data for both the annealed and unannealed samples after they have been normalized using the reference sample data. If the sample of interest does not produce any off specular scattering (like the P_0 reference sample) then the resulting $P_{Normalized}$ will be equal to 1 for all wavelengths. If however a suitable correlation lengthscale does exist in the system a polarization change (*i.e.* $P_{Normalized} \neq 1$) will be observed that has a strong wavelength dependence. An example of the 2D normalized SERGIS polarization data can be seen in **Figure 3** for the two representative samples of interest (*i.e.* annealed and unannealed).

The SERGIS signals from both an as-cast and an annealed sample have been measured and compared, as shown in **Figure 4**. The unannealed sample contained no structural correlations on the length scales that the spin-echo measurement is sensitive to and so produces a flat line at a 0.0 (a normalized polarization of 1). In contrast the annealed sample starts at 0.0 and there is a significant decay in the polarization as the spin-echo length increases before reaching a plateau that begins at approximately 1,200 nm. If the data is considered in a similar manner to Spin Echo Small Angle Neutron Scattering data from a dilute solution of particles then the data is consistent with a maximum average particle diameter of approximately 1,200 nm with no near neighbors.

Copyright © 2014 Journal of Visualized Experiments

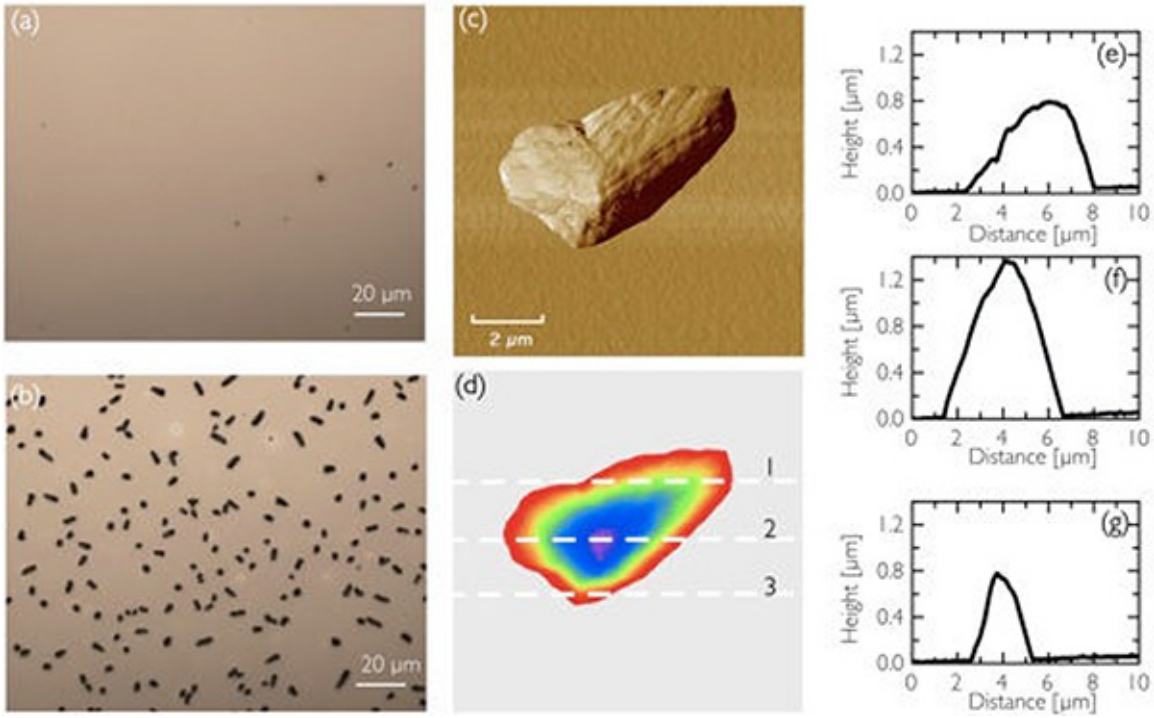

Figure 1. Optical microscopy images of the P3HT-PCBM film (a) before annealing and (b) after annealing at 150 °C for 1 hr. A higher magnification AFM phase image of one of the PCBM crystallites present after annealing is also shown in (**c**), and height section analysis for the same PC60BM crystallite at 3 different positions on the crystallite indicated as 1, 2, and 3 on (**d**) are shown in (**e**) 1, (**f**) 2, and (**g**) 3. Reprinted with permission from *Appl. Phys. Lett.* **102**, 073111, http://dx.doi.org/10.1063/1.4793513 (2013). Copyright 2013, AIP Publishing LLC. Click here to view larger image.

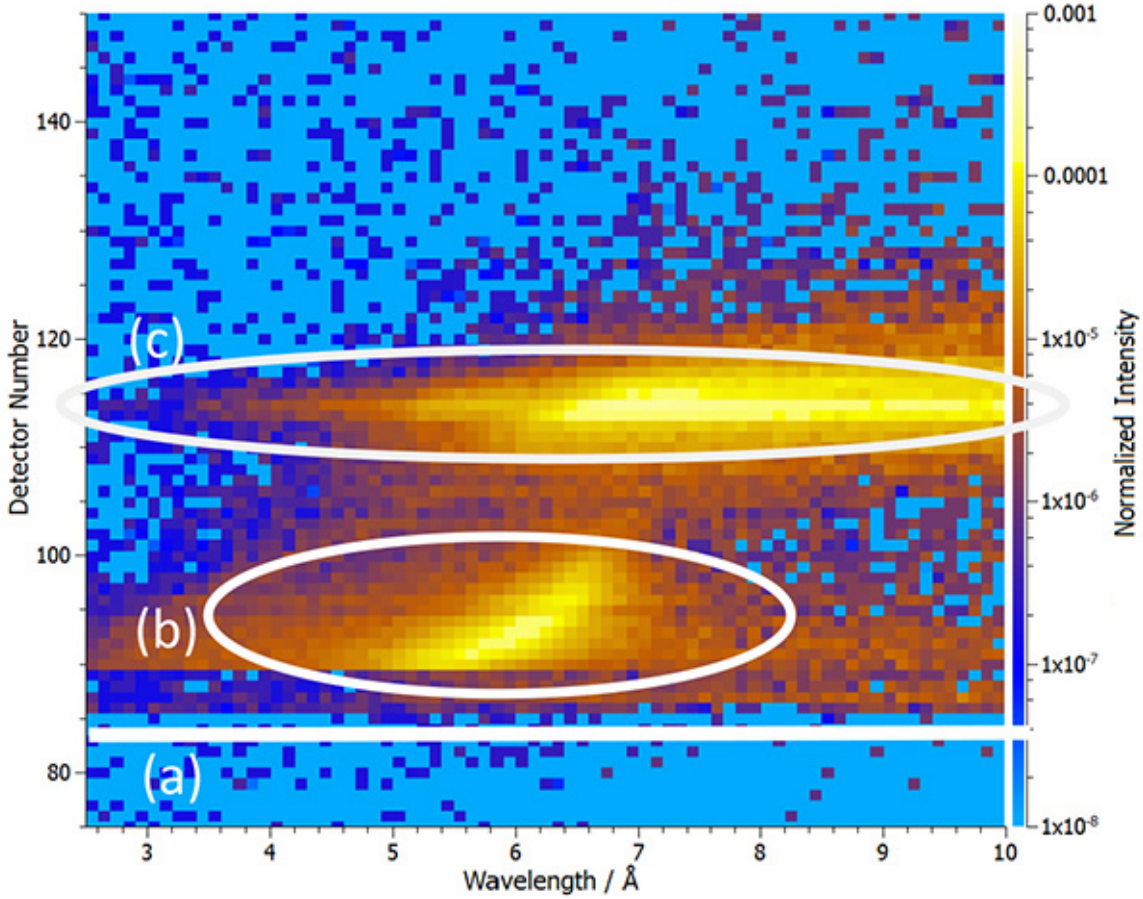

Figure 2. The normalized spin up reflectivity from the annealed P3HT/PCBM sample. The position that the direct beam would have appeared at had it not been blocked is indicated by the white line (**a**), the refracted beam is indicated by (**b**), and the specular reflection is indicated by (**c**). Reprinted with permission from *Appl. Phys. Lett.* **102**, 073111, http://dx.doi.org/10.1063/1.4793513 (2013). Copyright 2013, AIP Publishing LLC. Click here to view larger image.

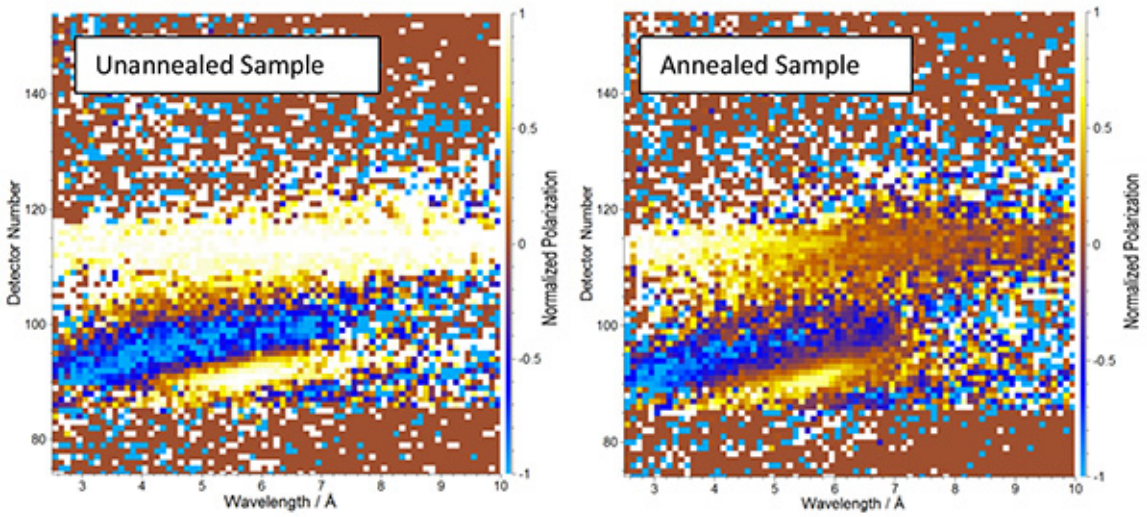

Figure 3. 2D normalized polarization images of the unannealed and annealed sample as a function of reflection angle and wavelength. Detector number 114 is the position of the specular reflection. Click here to view larger image.

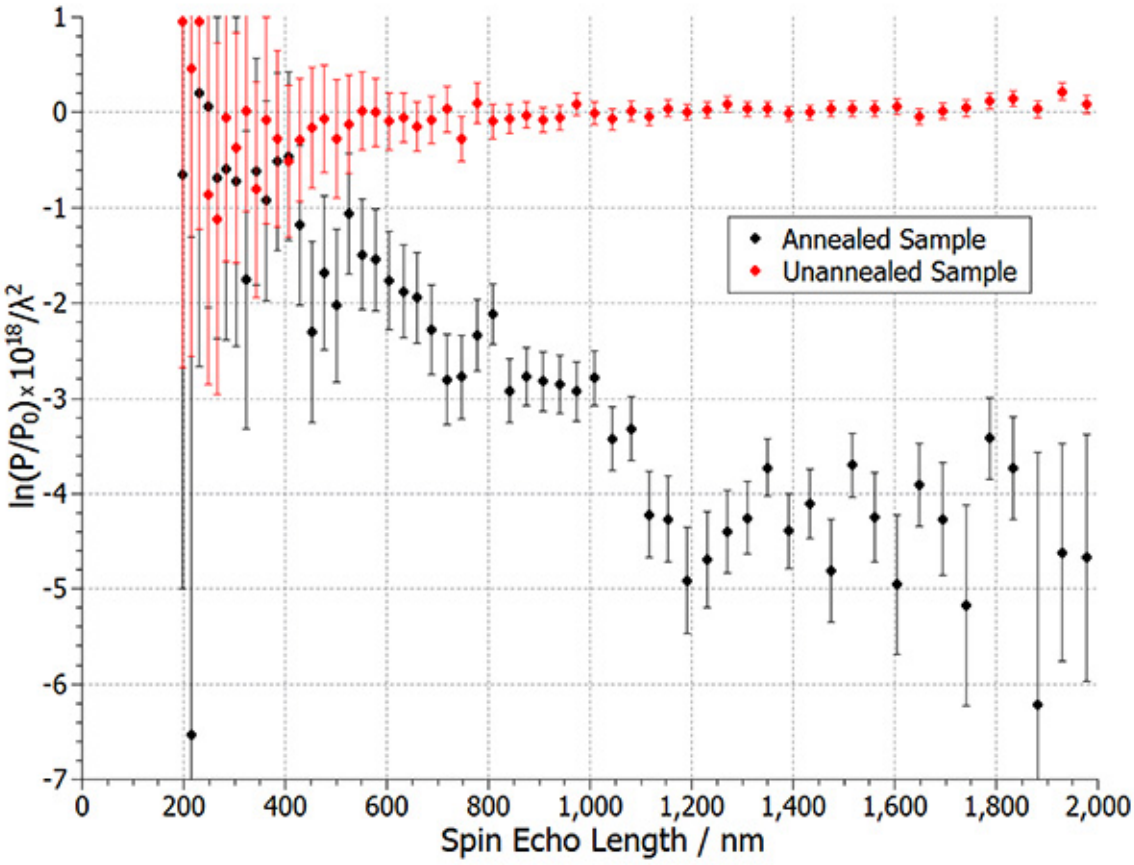

Figure 4. SERGIS data for the annealed and unannealed sample showing distinct polarization and a plateau starting at approximately 1,200 nm in the annealed sample and an effective zero polarization in the unannealed sample. The SERGIS signal was calculated by integrating **Figure 3** between detector pixels 110 and 118, which falls either side of and incorporates the specular reflection at detector pixel 114. Reprinted with permission from *Appl. Phys. Lett.* **102**, 073111, http://dx.doi.org/10.1063/1.4793513 (2013). Copyright 2013, AIP Publishing LLC. Click here to view larger image.

Discussion

The microscopy data in **Figure 1** clearly shows that before annealing the P3HT:PCBM thin film is flat and smooth and after thermal annealing there are many large irregular PCBM crystallites present on the surface with lateral dimensions ranging between about 1-10 µm. This is attributed to PCBM migration towards the top surface of the film and subsequent aggregation to form large crystallites. A strong SERGIS signal associated with scattering from PCBM crystallites in the annealed sample is seen in **Figure 4**. If the data is considered in a similar manner to Spin Echo Small Angle Neutron Scattering data from a dilute solution of particles then the SERGIS experiment suggests an average maximum particle diameter of 1.2 µm which falls within the range derived from the microscopy data, therefore there is good agreement between the length-scale found by the SERGIS technique and that observed by microscopy.

For samples that contain relatively large well separated discrete structures, like the crystallites in the representative data presented here, the wavelength dependence of the polarization can be considered to consist of two distinct components: one due to structural correlations and the other due to the wavelength squared dependence of the neutron scattering length density. The latter does not add any useful information to the data and will mask the plateau in polarization expected in a strongly scattering sample. Therefore the procedural step 3.10 is used to remove the wavelength squared dependence of scattering length density in order to simplify interpretation of the SERGIS results. Whilst in general it is difficult to completely decouple form factor data from inter-particle structure data; for well separated discrete structures where the inter-particle data signal will be weak as presented here it is assumed that the SERGIS signal observed here is dominated by the particle size and shape.

In general, neutrons are weakly interacting particles and therefore, as with other neutron techniques, SERGIS is likely to be well suited to investigating buried structures (although not demonstrated here). Unlike other reflectivity techniques that probe the sample as a function of depth, the SERGIS technique has the advantage that it can probe structures in the plane of the sample surface. The full experimental capabilities of the SERGIS technique are still being determined and is an area of continued research.

In comparison to scattering observed in neutron reflection measurements the SERGIS signals are often weak and are unlikely to be observed on current instrumentation if the in-plane structures within the sample under investigation are dilute, disordered, small in size and polydisperse

or the neutron scattering contrast is low. Therefore, the SERGIS technique is limited to measuring samples that contain a high density of moderately sized features (30 nm to 5 μm), which scatter neutrons strongly, or samples wherein the features of interest are arranged on a lattice.

One of the critical steps in any SERGIS experiment is selecting a suitable reference sample. Ideally it should have an extremely extended critical reflection region in order to permit good counting statistics to be acquired relatively quickly. Also, the reference sample should be as flat as possible and should not produce any off-specular scattering, this ensures that it will not depolarize or broaden the neutron beam. For the representative results presented here an optically flat, clean piece of amorphous quartz was used to collect the P0 data set. Likewise the samples of interest are fabricated on thick silicon substrates to eliminate any possibility of the wafer bending during the thin film drying process, thereby ensuring optimum flatness of the samples. Another critical step is the selection of a suitable area for the integration within the normalized 2D data set produced. This area should be selected so as to avoid swamping the desired SERGIS signal by any potential polarization inhomogeneities resulting from imperfections in the field line-integrals. The available Q space that the SERGIS signal may be integrated over is effectively limited to a series of discrete Q values at any given spin-echo length configuration.

Obviously the cost and time required to measure sample structures by the SERGIS technique is considerably greater than microscopy techniques used to corroborate the data presented here. However, the use of SERGIS to probe irregular particles sitting on the surface of a thin film clearly has been demonstrated. In the future this technique will hopefully be able to investigate buried structure. The weakly interacting nature of neutrons should permit them to penetrate through samples, and depolarize at buried interfaces. Therefore, the important advantage that SERGIS may have over other techniques is that it should be able to characterize similar features and effects when they are buried, unlike microscopy based techniques, which are typically limited to surface structures. Hopefully in the future it will be possible to use SERGIS to look at the effect of annealing on PCBM crystallite growth within a polymer solar cell that has been completed with a metallic cathode and encapsulating layer, in contrast to the incomplete device structures presented here.

Disclosures

The author Robert Dalgliesh is an employee of the ISIS Pulsed Neutron and Muon Source that hosts the instrument used in this experiment.

Acknowledgements

AJP was funded by the EPSRC Soft Nanotechnology platform grant EP/E046215/1. The neutron experiments were supported by the STFC via the allocation of experimental time to use OffSpec (RB 1110285).

References

1. Mezei, F. Neutron spin echo: A new concept in polarized thermal neutron techniques. *Zeitschriftfür Physik A Hadrons Nuclei*. **255,** 146-160 (1972).
2. Falus, P., Vorobiev, A. and Krist, T. Test of a two-dimensional neutron spin analyzer. *Physica B Condens. Matter. Mater. Phys.* **385-386,** 1149-1151 (2006).
3. Ashkar, R., *et al.* Dynamical theory calculations of spin-echo resolved grazing-incidence scattering from a diffraction grating. *J. Appl. Crystallogr.* **43**(3), 455-465 (2010).
4. Ashkar, R. *et al.* Dynamical theory: Application to spin-echo resolved grazing incidence scattering from periodic structures. *J. Appl. Phys.* **110(10),** 102201 (2011).
5. Pynn, R., Ashkar, R., Stonaha, P., Washington, A.L.,Some recent results using spin echo resolved grazing incidence scattering (SERGIS). *hysica B Condens. Matter. Mater. Phys.* **406**(12), 2350-2353 (2011).
6. Ashkar, R. *et al.* Spin-Echo Resolved Grazing Incidence Scattering (SERGIS) at Pulsed and CW Neutron Sources. *J. Phy. Conf. Ser.* **251**(1), 012066 (2010).
7. Vorobiev, A. *et al.* Phase and microphase separation of polymer thin films dewetted from Silicon-A spin-echo resolved grazing incidence neutron scattering study. *J. Phys. Chem. B.* **115**(19), 5754-5765 (2011).
8. Major, J. *et al.* A spin-echo resolved grazing incidence scattering setup for the neutron interrogation of buried nanostructures. *Rev. Sci. Instrum.* **80** (12), 123903 (2009).
9. Parnell, A.J., Dalgliesh, R.M., Jones, R.A.L., and Dunbar, A.D.F., A neutron spin echo resolved grazing incidence scattering study of crystallites in organic photovoltaic thin films. *Appl. Phys. Lett*. **102**, 073111 (2013).
10. Dalgliesh, R.M., Langridge, S., Plomp, J., De Haan, V.O., Van Well, A.A. Offspec, the ISIS spin-echo reflectometer. *hysica B Condens. Matter. Mater. Phys.* **406** (12), 2346-2349 (2011).
11. Krouglov T., de Schepper I. M., Bouwman W. G. and Rekveldt M. T. Real-space interpretation of spin-echo small-angle neutron scattering. *J. Appl. Crystallogr* . **36**, 117-124 (2003).
12. Brady, M. A., Su, G.M. and Chabinyc, M.L. Recent progress in the morphology of bulk heterojunctionphotovoltaics. *Soft Matter.* **7**(23), 11065-11077 (2011).
13. Huang, Y.-C. *et al.* Study of the effect of annealing process on the performance of P3HT/PCBM photovoltaic devices using scanning-probe microscopy. *Solar Energy Mater. Solar Cells.* **93**(6-7), 888-892 (2009).
14. Parnell, A.J., *et al.* Depletion of PCBM at the Cathode Interface in P3HT/PCBM Thin Films as Quantified via Neutron Reflectivity Measurements. *Adv. Mater.* **22**(22), 2444-2447 (2010).

Copyright © 2014 Journal of Visualized Experiments